Integrated single emitters under cryogenic conditions

Universität Stuttgart

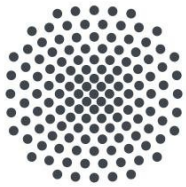

Universität
Stuttgart

Vladislav Bushmakin

01.01.2020

Abstract

Abstract goes here

Dedication

To mum and dad

Declaration

I declare that..

Acknowledgements

I want to thank...

Contents

Chapter 1

Introduction

Chapter 2

Theory

We want to discuss: bloch equations(on demand single photon source) single photon statistics A). Fourier limited emitter. LUMO, HOMO. Broadening

B). dipolar emission fiber microlense optics(collection of photons) fibers as waveguides(cross polarization stipulation) nanowaveguides C). stark-shift for energy shift interference of photons

2.1 Photophysics of fluorescent molecules

The discovery of the association of spectra and chemical elements by R.Bunsen and G.Kirchhoff have opened the way for classification of microscopic consistency of matter. For example, the study of the Fraunhofer lines has revealed the consistency of the Sun[1]. However, only in 1989, a spectroscopic line could be attributed not to an ensemble of elements, but a single molecule in a solid by W.E.Moerner and L.Kador [2]. Such a pioneering experiment was a result of increased interest to molecular spectroscopy started from the 1970s after the discovery of the spectral hole-burning technique[3, 4]. Later, the idea of fluorescence excitation spectroscopy, i.e. observation of the intensity of emission versus the frequency of excitation, introduced by M.Orrit in 1990 [5] has facilitated the detection of individual molecules. The single molecules spectroscopy has significantly advanced for the last three decades[Ilja, Vahid et al...]; however, the basic understanding of the molecular spectra remained intact. Thus, this chapter is dedicated to the theoretical foundation of the spectroscopy of a single-molecule.

To understand the constituents of the spectrum of a molecule, its electronic eigenstates can be represented by the Jablonsky diagram Fig. A[6]. First, assuming a molecule is isolated from a host, the electronic, vibronic and phononic transitions would form the spectra of a molecule.

At low temperatures, the molecules are initialized in the first electronic and vibronic state, which is usually a single state. Hence the first excited electronic state is a singlet state due to the conservation of spin. From the first excited state, the electron can transit to the long-lived triplet state by intersystem crossing (ISC), what would render a molecule "dark". The spontaneous decay from the excited state can proceed by via two channels: the internal conversion, i.e. the direct transition to the ground state; or the fluorescence — the decay to one of the vibronic states of the system's ground state with consequent rapid (sub-picosecond range) relaxation to the system's ground state.

The relative intensity of the spectral lines of a molecule is determined by the overlap of the vibrational wavefunctions of the ground and excited state. The more this wavefunctions overlap — the higher the intensity of a transition. This is a so-called Frank-Condon principle, which states that the electronic transition is much faster than the time for the nuclei to reconfigure. As a result, the electronic transitions between excited and ground states can be represented as vertical transitions on the Fig.BB. The integral overlap between the vibrational states of the excited and ground state is referred to as the Frank-Condon factor.

Oftentimes the transition of interest is the *zero-phonon line,* which corresponds to a coherent scattering. Hence rigid molecules are preferred, which nuclei configuration stays the same during the excitation process. The Frank-Condon factor for such molecules would be close to unity.

So far, we assumed a molecule isolated from a matrix. Though, the optical properties of organic molecules embedded in organic solids can vary depending on the structure of both a guest and a host molecule. The host matrix bandstructure stems from the constituent molecules' close packing, and its excited states spread over an ensemble of molecules. However, the guest molecules excited states are localized and decoupled from the host matrix what renders its spectral lines narrow. The coupling of the molecule's electron with the solid's phonons gives rise to the *phonon wing* observed in the spectra*.* The Debye-Waller factor describes the extent of electron-phonon coupling in a crystal, i.e. accounts for the inelastic scattering within a crystal: $\alpha_{DW} = \frac{I_{ZPL}}{I_{ZPL}+I_{phonon}}$.

Hence, taking into account the molecular transitions and the transitions stemming from the interaction with lattice vibrations the resulting spectra of a molecule in a crystal can be schematically represented, as on the figure 2 and g.

However, a host matrix is not only giving rise to new decay channels, but also determines the resonant of a molecule. Depending on the 1? 1 the resonant frequency changes. For example, DBT in anthracene and DBT in naphthalene exhibit different resonant frequencies.

Another effect introduced by the host matrix is the inhomogeneous broadening of the molecules zero-phonon lines: the molecules in the host matrix would experience different nanoenvironment and the further the host matrix from an ideal crystal lattice, the broader the inhomogeneous broadening, as illustrated on the fig A and B. The inhomogeneous broadening plays a significant role in this thesis, as will be seen in the fiber-coupling chapter.

2.2 Modeling light-molecule interaction

In order to gather control over the molecular emission the interaction of a molecule with a light pulse has to be modeled. The conventional approach is to solve optical Bloch equation describing the two-level system population dynamics. However, a molecule in a solid matrix cannot be treated as a closed system, hence requires a model involving coupling to the environment. ===Bloch-Redfield?=== The dynamics of a molecule in environment can be described as an open system in terms of density matrices via Lindblad master equation[**?**].

OR

The field of quantum optics and photonics has experienced a fast evolution for the past two decades. The advances in atomic physics [] alongside with the discov-

ery of the parametric down-conversion process [] have facilitated the first studies on the nature of single photons. The breakthroughs, like the first observations of anti-bunched light by J. Clauser in 1973 [1], the violation of Bell inequalities by A. Aspect in 1982 and the interference of a pair of single photons on a beam splitter by Hong, Ou and Mandel in 1987 [2] have emphasised the quantum properties of photons. The development of spectroscopy of the crystalline and amorphic organic host matrices with guest molecules[Hole burning; Shpolskiy] set the foundation for the pioneering experiments in the solid-state single-photon sources[Moerer; Orrit]. The breakthroughs in quantum cryptography[Ekkert] and quantum computing with photons[KLM] mentioned in the Introduction served a strong stimulus for the development of the field. The discovery of the single colour centres in crystalls[] and the quantum dots[] have open the prospect of employing the large scale semiconductor manufacturing technologies for the upcoming quantum revolution.

However, despite the significant advances in the single-photon generation, no clear leader has been established hitherto.

This chapter aims to review the current state-of-the-art in the solid-state single-photon generation and highlight the place of organic dye molecules in the future of quantum photonics. For completeness of the discussion, the chapter starts with an introduction to single emitter photophysics and the keys requirements for an ideal single-photon source are outlined.

Before discussing the photon statistics of a single emitter, we overview the quantum description of light-matter interaction. As the main advantage of single emitters over other single-photon sources is the option of on-demand photon generation. The control over photon emission of an atom is made possible by the excited state population's coherent driving with a strong field. This behavior of the excited state population is called Rabi oscillations. Besides, driving a system with a short pulse called $\pi pulse can enable on-demand photon generation. Such a pulse reverses an atom's population with a follow$

2.2.1 Jaynes-Cummings model

However, as in this thesis, we consider molecules embedded into a solid matrix, the influence of the host, alongside the laser field and vacuum, has to be discussed.

The interaction of an atom with the quantized electromagnetic field can be described by the Jaynes-Cummings model.

The Jaynes-Cummings hamiltonian yields:

$\hat{H} = \hat{H}_F + \hat{H}_A + \hat{H}_{AF}$

In the second quantization the atomic part of the Hamiltonian:

$\hat{H}_A = \hbar\omega_A[\hat{\sigma}_+, \hat{\sigma}_-]$,

where ω_A - the frequency corresponding to the transition between ground and excited state of the atom; and $\hat{\sigma}_+ = |e\rangle\langle g|$; $\hat{\sigma}_- = |g\rangle\langle e|$ — rising and lowering atomic operators.

The field part, as we consider only the single mode of the field:

$\hat{H}_F = \hbar\omega_C(\hat{a}^\dagger\hat{a} + \frac{1}{2})$,

where $\hat{a}^\dagger$ and $\hat{a}$ are the bosonic creation and annihilation operators, ω_C — the field mode frequency.

And finally the interaction of the atom as a dipole with the a field :

$\hat{H}_{AF} = -\hat{\vec{d}}\hat{\vec{E}}(\vec{R})$

what in the case of a two-level atom and a single mode field can be expressed as:

$\hat{H}_{AF} = \hbar\frac{\Omega}{2}(\hat{a}^\dagger + \hat{a})(\hat{\sigma}_+ + \hat{\sigma}_-)$,

where Ω is the vacuum Rabi frequency.

Hence, the hamiltonian of atom-field interaction yields:

$\hat{H} = \hbar\omega_C(\hat{a}^\dagger\hat{a} + \frac{1}{2}) + \hbar\omega_A[\hat{\sigma}_+, \hat{\sigma}_-] + \hbar\frac{\Omega}{2}(\hat{a}^\dagger + \hat{a})(\hat{\sigma}_+ + \hat{\sigma}_-)$

Rotating wave approximation:

In the interaction picture, the hamiltonian can be simplified by transforming into the co-rotating frame. If we set $\hat{H}_0 = \hat{H}_A + \hat{H}_F$, it yields:

$\hat{H}_{AF}(t) = e^{i\hat{H}_0 t/\hbar}\hat{H}_{AF}e^{-i\hat{H}_0 t/\hbar}$,

and hence the operators $\hat{a}$ and $\hat{a}^\dagger$ would evolve as $\hat{a}(t) = \hat{a}(0)e^{-i\omega_C t}$; $\hat{a}^\dagger(t) = \hat{a}^\dagger(0)e^{-i\omega_C t}$;

the operators $\hat{\sigma}$ and $\hat{\sigma}^\dagger$ as $\hat{\sigma}_\pm(t) = \hat{\sigma}_\pm(0)e^{\pm i\omega_A t}$;

For the last term in $\hat{H}$ in the interaction picture the products are as follows:

$\hat{\sigma}_+\hat{a} \sim e^{i(\omega_A - \omega_C)t}$

$\hat{\sigma}_-\hat{a}^\dagger \sim e^{-i(\omega_A - \omega_C)t}$

$\hat{\sigma}_+\hat{a}^\dagger \sim e^{i(\omega_C + \omega_A)t}$

$\hat{\sigma}_-\hat{a} \sim e^{-i(\omega_C + \omega_A)t}$

Near the resonance ($\omega_C \approx \omega_A$) the highly oscillating terms ($\hat{\sigma}_-\hat{a}$ and $\hat{\sigma}_+\hat{a}^\dagger$) can be omitted. This approximation is called *rotating wave approximation*.

The transforming back to the Schrödinger picture resulting hamiltonian yields:

$\hat{H}_{AF}(t) = e^{-i\hat{H}_0 t/\hbar}\hat{H}_{AF}e^{i\hat{H}_0 t/\hbar}$

$\hat{H} = \hbar\omega_C(\hat{a}^\dagger\hat{a} + \frac{1}{2}) + \hbar\omega_A[\hat{\sigma}_+, \hat{\sigma}_-] + \hbar\frac{\Omega}{2}(\hat{\sigma}_-\hat{a}^\dagger + \hat{\sigma}_+\hat{a})$

Dressed states; Mollow tripplet

The zero-point energy can be neglected, thus the hamiltonian simplifies to:

$\hat{H} = \hbar\omega_C\hat{a}^\dagger\hat{a} + \hbar\omega_A[\hat{\sigma}_+, \hat{\sigma}_-] + \hbar\frac{\Omega}{2}(\hat{\sigma}_-\hat{a}^\dagger + \hat{\sigma}_+\hat{a})$,

An operator for the number of excitations can be expressed as:

$\hat{N}_e = [\hat{\sigma}_+, \hat{\sigma}_-] + \hat{a}^\dagger\hat{a} = |e\rangle\langle e| + \hat{a}^\dagger\hat{a}$,

this operator commutes with the hamiltonian of the system

$[\hat{N}_e, \hat{H}] = 0$, hence the eigenstates of $\hat{N}_e$ form the basis in the system's Hilbert space.

The hamiltonian of the system in this basis forms a block diagonal matrix with matrices $\hat{H}_n$ and the total energy shift by $\frac{1}{2}\hbar\Delta$:

$$\hat{H}_n = \begin{bmatrix} n\hbar\omega_C - \frac{1}{2}\hbar\Delta & \frac{\sqrt{n\hbar\Omega}}{2} \\ \frac{\sqrt{n\hbar\Omega}}{2} & n\hbar\omega_C + \frac{1}{2}\hbar\Delta \end{bmatrix}$$

This matrix fully describes the hamiltonian, as only states with ± 1 photon number changes are coupled.

The energy eigenvalues of $\hat{H}_n$:

$E_{n,\pm} = \left(n\hbar\omega_c - \frac{1}{2}\hbar\Delta\right) \pm \frac{1}{2}\hbar\sqrt{\Delta^2 + n\Omega^2}$

And the eigenstates are:

$|n,+\rangle = \cos\left(\frac{\Theta_n}{2}\right)|e, n-1\rangle + \sin\left(\frac{\Theta_n}{2}\right)|g, n\rangle$

$|n,-\rangle = \cos\left(\frac{\Theta_n}{2}\right)|g, n\rangle - \sin\left(\frac{\Theta_n}{2}\right)|e, n-1\rangle$

where $\tan\Theta_n = -\frac{\sqrt{n}\Omega}{\Delta}$.

This states are also referred to as dressed states, as they display the AC Stark shift due to atom-field interaction.

2.2.2 Lindblad master equation

However, the Jaynes-Cummings Hamiltonian only describes photon-atom interaction, but spontaneous emission and interaction with the surrounding phonon bath also should be accounted for.

Hence, to describe the dynamics of a system realistically it has to be treated as an open system. First, it is necessary to represent the state of a quantum system in terms of density matrices instead of state vectors. As the density matrix description accounts for the mixed states, inevitable in treatment of open quantum systems.

Definition of density matrix:

$\rho = \sum_j p_j \left|\psi_j\right\rangle \left\langle\psi_j\right|$

A general approach to describe open quantum systems is to use Lindblad equations:

$\frac{d}{dt}\rho = -i[H,\rho] + \sum_k \Gamma_k \left(L_k \rho L_k^\dagger - \frac{1}{2}\left\{L_k L_k^\dagger, \rho\right\}\right) \equiv \mathcal{L}\rho$

Some explanation of LIndblad equations and how it encorporates the coupling to the bath. Basics for understanding the QuTip simulation setup.

2.2.3 Spectrum of a two-level system

2.3 Photon statistics of a single emitter

2.3.1 Second order coherence function

2.3.2 Photon waiting time distribution

2.4 Emission collection strategies

The critical advantage of single emitters stems from the prospects of on-demand single-photon generation. However, its practical realisation significantly depends both on the quantum yield of an emitter and the efficiency to collect the scattered photons. Mainly two approaches are pursued: to use high refractive index optical elements, such as solid immersion lenses to direct the mode of emission into the collection optics[], and to build a cavity around an emitter enforcing it to emit in a defined mode[]. Both strategies able to improve the collection of photons emitted by an organic molecule[], yet only the geometric approach is considered in this thesis. Hence, this chapter only briefly overviews the cavity QED approaches as a prospect for further collection efficiency improvements. Before a discussion of collection strategies, the overall efficiency has to be specified.

The total efficiency of on demand generation of indistinguishable single photons can be expressed as follows: $\eta_{totall} = p_{exc} \times \eta_{yield} \times \alpha_{transition} \times \beta_{mode} \times (1 - g^2(0)) \times \eta_{collection}$,

In the previous chapter, we reviewed the nature of coefficients α, η_{yield} and p_{exc} and their approximate values for various emitters. Although this chapter is mostly devoted to the strategies of improving $\eta_{collection}$ and β_{mode}, the emission enhancement enabled by cavity QED approaches will be mentioned.

2.4.1 Dipole at a dielectric interface

$NA = n_{medium} \sin\Theta$

The spontaneous emission of an emitter in an isotropic medium is distributed among the whole 4π. Hence an efficient collection of photons as high NA setup as possible. At the same time, the NA of an objective is constrained by the n_{medium} between the objective and the sample if no additional strategy is applied.

The approach which is often followed at room temperature microscopy is to immerse the sample into the immersion oil with high refractive index[] n_{oil}, what significantly increases NA. An even better result can be achieved with the use of a solid immersion lens — a hemisphere made out of transparent material with a high refractive index, such as ZrO2 (2.18) or diamond (2.41?). The principle behind the SIL lens is the same as of the immersion oil microscope, hence the effective NA can be improved. Thus, the effective NA of a microscope with a solid immersion lens can be expressed as:

$NA = NA_{obj} \times n_{SIL}$

$NA = n_{medium} \sin \Theta$

The spontaneous emission of an emitter in an isotropic medium is distributed among the whole 4π. Hence an efficient collection of photons as high NA setup as possible. At the same time, the NA of an objective is constrained by the n_{medium} between the objective and the sample if no additional strategy is applied.

The approach which is often followed at room temperature microscopy is to immerse the sample into the immersion oil with high refractive index[] n_{oil}, what significantly increases NA. An even better result can be achieved with the use of a solid immersion lens — a hemisphere made out of transparent material with a high refractive index, such as ZrO2 (2.18) or diamond (2.41?). The principle behind the SIL lens is the same as of the immersion oil microscope, hence the effective NA can be improved. Thus, the effective NA of a microscope with a solid immersion lens can be expressed as:

$NA = NA_{obj} \times n_{SIL}$

2.4.2 Free space collection

$NA = n_{medium} \sin \Theta$

The spontaneous emission of an emitter in an isotropic medium is distributed among the whole 4π. Hence an efficient collection of photons as high NA setup as possible. At the same time, the NA of an objective is constrained by the n_{medium} between the objective and the sample if no additional strategy is applied.

The approach which is often followed at room temperature microscopy is to immerse the sample into the immersion oil with high refractive index[] n_{oil}, what significantly increases NA. An even better result can be achieved with the use of a solid immersion lens — a hemisphere made out of transparent material with a high refractive index, such as ZrO2 (2.18) or diamond (2.41?). The principle behind the SIL lens is the same as of the immersion oil microscope, hence the effective NA can be improved. Thus, the effective NA of a microscope with a solid immersion lens can be expressed as:

$NA = NA_{obj} \times n_{SIL}$

2.4.3 Fiber coupling

Before the discussion on the methods to couple light into optical fibers, we have to a). $_{d}iscusshowemitters emit, and b).whataretherequirements for the light to propagate in the fiber.$

We have discussed in the previous paragraph how the emission pattern of a dipole changes near a dielectric interface, and we figured out that light is being captured into the hemisphere with a higher refractive index, in addition the shape of the emission changes dramatically, what will influence the overlap of the emission mode and the mode propagating in a fiber.

The chapter is dedicated to the review of the theory of single mode fibers and

Chapter 3

Experimantal setup

3.1 Free space experimental setup

3.2 Fiber-coupled experimental setup

Chapter 4

Alignment free fiber coupled SPS

4.1 Bare fiber tip coupling

4.2 On-tip collection optics

4.3 Outlook

Chapter 5

Pulse-induced transparency

5.1 Experimental observations

5.2 Simulation results

5.3 Outlook

Chapter 6

Emitter efficiency estimation with photon statistics

6.1 Waiting time distribution

6.2 Deduction of emitter's efficiency

6.3 Outlook

Chapter 7

Conclusions